Recognition of histone H3 methylation states by the PHD1 domain of histone demethylase KDM5A

James E Longbotham[1], Mark J S Kelly[2*], Danica Galonić Fujimori[1,2,*]

[1] Department of Cellular and Molecular Pharmacology, University of California San Francisco, 600 16th Street, Genentech Hall, San Francisco, California 94158, USA.

[2] Department of Pharmaceutical Chemistry, University of California San Francisco, 600 16th Street, Genentech Hall, San Francisco, California 94158, USA

*Corresponding authors: Danica.Fujimori@ucsf.edu, Mark.Kelly@ucsf.edu

Abstract

PHD reader domains are chromatin binding modules often responsible for the recruitment of large protein complexes that contain histone modifying enzymes, chromatin remodelers and DNA repair machinery. PHD domains recognize N–terminal residues of histone H3 and are sensitive to the methylation state of Lys4 in histone H3 (H3K4). Histone demethylase KDM5A, an epigenetic eraser enzyme that contains three PHD domains, is often overexpressed in various cancers and its demethylation activity is allosterically enhanced when its PHD1 domain is bound to the H3 tail. The allosteric regulatory function of PHD1 expands roles of reader domains, suggesting unique features of this chromatin interacting module. Our previous studies determined the H3 binding site of PHD1, although it remains unclear how the H3 tail interacts with the N–terminal residues of PHD1 and how PHD1 discriminates against H3 tails with varying degrees of H3K4 methylation. Here we show that the N–terminal region of PHD1 is initially unstructured, but becomes ordered upon binding of the high affinity H3 peptide ligands. We also observe differential interactions of conserved binding residues with differently methylated H3K4 peptides (me0, me1, me2 or me3), providing a rational for this PHD1 domain's preference for lower methylation states of H3K4. We further assessed the contributions of various H3 interacting residues in the PHD1 domain to the binding of H3 peptides using mutagenesis. The insights into the H3 binding site could provide useful information to aid development of allosteric small molecule modulators of KDM5A.

Introduction

Histone modifications play a central role in regulating chromatin structure and function. Protein reader domains recognize specific histone modifications and are often responsible for recruiting large protein complexes that contain histone modifying enzymes, chromatin remodelers and DNA repair machinery[1]. Plant homeodomain (PHD) domains are specific for recognizing the N–terminal residues of histone H3 and read the methylation state of H3K4 and, to a lesser extent, H3R2[2]. While the majority of PHD domains recognize H3, recognition of H4 peptides has been observed in extended PHD domains in MLL3/4[3,4].

The conserved PHD fold consists of a two strand β–sheet, a C–terminal α–helix and two structural zinc atoms stabilized by a Cys4–His–Cys3 motif[2]. Depending on the residues involved, different PHD domains preferentially engage H3 as a function of the methylation status of H3K4. H3K4me3 preferring PHD domains, such as BPTF[5] and TAF3[6], have two to four aromatic residues that form an aromatic cage in the H3K4 binding pocket which allows for cation–π interactions with tri–methylated H3K4[7] (**Figure 1a**). Inclusion of a H3K4 interacting glutamate residue in the aromatic cage of PHF20–PHD leads to the specificity for H3K4me2[8]. PHD domains that preferentially bind unmodified H3K4, such as BHC80[9] and AIRE[10,11], lack an aromatic cage, but instead have a H3K4 binding pocket consisting of both acidic and hydrophobic residues. Specificity for unmodified H3K4 is achieved by electrostatic and hydrogen bond interactions. These domains discriminate against methylated H3K4 residues by steric occlusion of H3K4 methyl groups from the binding pocket in addition to an increase in cationic radius and decrease in hydrogen bond potential[9–14].

Members of the KDM5 family are H3K4me3 specific demethylases and contain varying number of PHD domains. All four members of the KDM5 family are involved in pathogenesis and progression of various cancers[15–30] and other, particularly neurological, disorders[31,32]. For this reason there is significant interest in developing therapeutics targeting these enzymes[33–37]. KDM5A specifically is overexpressed in breast cancer, where it promotes cancer progression and metastasis[38], and there is evidence for its role in resistance to

endocrine therapy[39] as well as cancer drug resistance in lung cancer models[40]. KDM5A contains three PHD domains. Its PHD3 domain is specific for H3K4me3 and it is thought to be responsible for recruiting KDM5A to the site of its substrate. PHD3 is also known to form a fusion with NUP98 in acute leukemia[15]. We have previously shown that the PHD1 domain preferentially binds unmodified H3[41] and that the engagement of the PHD1 domain with its ligand allosterically enhances the demethylation activity of KDM5A by stabilizing substrate binding to the catalytic domain[42]. Despite the importance of PHD1 in the demethylase activity of KDM5A, there is limited structural information on how its PHD1 domain interacts with H3 and how it can discriminate against the methylation states of H3K4 peptides. We have previously mapped the unmodified H3 peptide binding site of PHD1 using NMR[41]. Also important structural insights have been gained from studies performed on the PHD1 domain of homologue KDM5B[12,13]. However, questions remain about the interactions of the N–terminal region of the PHD1 domain, which was absent in the construct used in our previous NMR studies, as well as how peptide binding residues of this reader domain interact with methylated H3 peptides.

Here we show that the N–terminal segment of PHD1 is flexible and becomes structured upon peptide binding and that residues in this region interact strongly with the peptide. These interactions are modulated by the methylation status of H3K4, as we observe differential engagement of this region with differently methylated peptides. Peptide binding residues in PHD1 were further probed through mutagenesis. Structural information of this regulatory reader domain will contribute to knowledge of how PHD domains interact with their ligands. Additionally, given the allosteric role of this domain in regulation of KDM5A catalysis, structural information could assist in the development of unique allosteric small molecule ligands for use as chemical tools. This would allow for pharmacological interrogation of the role of this enzyme in KDM5A dependent disorders.

Methods

Expression and purification of WT and variant GST–PHD1.

WT and variant PHD1 constructs (S287–K347) were cloned into a pET41a vector and expressed in BL21(DE3) *E. coli* cells. Expression and purification of WT and variants followed the same protocol. Cells were induced with 0.4 mM IPTG and grown at 18 °C overnight before the pellet was collected. The cells were resuspended in lysis buffer (140 mM NaCl, 2.7 mM KCl, 10 mM Na_2HPO_4, 1.8 mM KH_2PO_4, 5 mM β–mercaptoethanol, 50 µM $ZnCl_2$, 1 mM phenylmethylsulfonyl fluoride (PMSF), pH 7.3), lysed by sonication and centrifuged. The supernatant was purified using Glutathione Sepharose 4B resin, washed with high salt buffer (50 mM HEPES, 700 mM KCl, 10% glycerol, 5 mM β–mercaptoethanol, 50 µM $ZnCl_2$, 1 mM PMSF, pH 8.0) and low salt buffer (50 mM HEPES, 150 mM KCl, 10% glycerol, 5 mM β–mercaptoethanol, 50 µM $ZnCl_2$, 1 mM PMSF, pH 8) and recovered by elution using low salt buffer supplemented with 30 mM glutathione. The sample was then further purified by size–exclusion chromatography using a Hiload 26/60 Superdex 75 gel filtration column in a buffer of 40 mM HEPES, 50 mM KCl, 5 mM β–mercaptoethanol, and 50 µM $ZnCl_2$, pH 8.0 concentrated and flash–frozen.

Fluorescence polarization binding assays.

The binding of GST–PHD1 to H3 10mer peptides was measured by either direct or competition–based fluorescence polarization (FP). For direct FP binding assay, 10 nM of C–terminal fluorescein labeled H3 10mer peptide were incubated for 30 mins with varying concentrations of GST–PHD1. Data from direct FP measurements were fitted to equation 1:

$$FP_{obs} = \frac{FP_{max}[PHD1] + FP_{min}K_d}{K_d + [PHD1]}$$

For competition–based FP assays, GST–PHD1, at a concentration equal to the K_d for unmodified H3 peptide, was incubated with 10 nM of C–terminal fluorescently labeled H3

10mer peptide and different concentrations of unlabeled peptides were used as competitors. Data from competition–based FP assays were fitted to equation 2:

$$FP_{obs} = \frac{K_i(FP_{max}[PHD1] + FP_{min}K_d) + FP_{min}K_d[I]}{K_i(K_d + [PHD1]) + K_d[I]}$$

where FP_{obs} is the observed FP, FP_{max} is the maximum FP value, FP_{min} is the minimum FP value, [PHD1] is concentration of GST–PHD1, K_d is the dissociation constant, K_i is the inhibition constant referring to the competing peptide and [I] is the competing peptide concentration.

Nuclear magnetic resonance experiments.

A PHD1 construct encompassing residues S287–E344 was used in NMR studies. The GST–PHD1 fusion construct was expressed in M9 minimal media containing ^{15}N ammonium chloride and/or $^{13}C_6$ D–glucose. The labelled GST–PHD1 was purified as described for binding studies with additional steps of removing the GST tag by TEV protease cleavage after elution from the Glutathione 4b resin. After cleavage the sample was incubated with nickel resin to remove the His–tagged TEV and the flow–through, containing the cleaved PHD1, was collected. Finally, the cleaved PHD1 was loaded onto a Hiload 26/60 Superdex 75 gel filtration column pre–equilibrated with 50 mM HEPES, 150 mM NaCl, 0.5 mM TCEP and 0.1 mM $ZnCl_2$ at pH 7.5.

150 µM ^{13}C–, ^{15}N–labelled PHD1 was used in 3D triple–resonance experiments for the backbone assignment of apo–PHD1. For the assignment of H3 10mer bound PHD1, 400 µM H3 10mer was added to the sample. HNCACB (pulse program: hncacbgpwg3d, TopSpin1.3p18) and CBCA(CO)NH (pulse program: cbcaconhgpwg3d, TopSpin1.3p18) experiments were recorded with a Bruker 500 MHz AVANCE DRX500 spectrometer equipped with an actively shielded Z–gradient QCI cryoprobe ($^{15}N/^{13}C/^{31}P$, ^{1}H). The 3D spectra were processed in NMRPipe and proton chemical shifts were referenced externally

to a DSS standard and while ^{13}C and ^{15}N chemical shifts were referenced indirectly to this value.

For 2D [^{15}N, ^{1}H]–HSQC peptide titration experiments, 200 µM ^{15}N–labeled PHD1 was used and spectra measured after each addition of H3 10mer peptides. The 2D (pulse program: fhsqcf3gpph, TopSpin1.3p18) spectra for the H3 10mer peptide titration series were recorded on a Bruker 800 MHz AVANCE–I spectrometer equipped with an actively shielded Z–gradient TXI cryoprobe. Chemical shift perturbations of HSQC peaks, upon addition of H3 10mer peptide, were calculated with the following equation:

$$\Delta\text{Chemical shift} = \sqrt{\frac{\Delta H^2 + (0.2\Delta N)^2}{2}}$$

All experiments were carried out at 298 K (calibrated with 4% v/v MeOH in MeOD) in 50 mM HEPES, 150 mM NaCl, 0.5 mM TCEP and 0.1 mM $ZnCl_2$ at pH 7.5 in 5% D_2O.

Results and Discussion

Unstructured N–terminal residues participate in H3 peptide recognition

PHD1 preferentially binds unmodified H3 peptides and the binding affinity decreases with an increase in H3K4 methylation[41,42]. Based on previous studies with the PHD1 domain of the demethylase KDM5B ($PHD1_{KDM5B}$), the predicted H3K4 binding pocket consists of conserved residues Asp292, Tyr294 and Leu310[12,13] (**Figure 1a,d**). We previously mapped the H3 peptide binding site of $PHD1_{KDM5A}$ domain using two–dimensional heteronuclear single quantum coherence (2D ^{15}N–HSQC) NMR titration experiments[41]. However, these experiments did not detect any interaction between the H3 peptide and a conserved H3K4 binding pocket residue, Asp292, in the PHD1 construct used (Asp292–Glu344). Our recent fluorescence polarization–based binding studies suggested that Asp292 is involved in binding when an N–terminally extended PHD1 construct (Ser287–Lys347) is used[42]. This observation prompted us to examine the contribution of these N–terminal residues to peptide binding and, additionally, to H3K4 methyl recognition.

In order to assess binding of the H3 peptide to PHD1, 2D ^{15}N HSQC experiments were conducted using a PHD1 (Ser287–Glu344) construct. The HSQC spectrum of apo PHD1 showed a well–dispersed set of peaks, consistent with a well–structured domain, which were assigned to individual residues using NMR triple–resonance backbone experiments (**Figure 1b**). Comparison of the HSQC spectra of Ser287–Glu344 with Asp292–Glu344, which we previously used, showed several overlapping peaks (**Supplementary Figure 1**), but a significant shift in many residues suggests structural differences between the two constructs. The H3 10mer peptide binding site in the Ser287–Glu344 PHD1 construct was identified by NMR peptide titration experiments (**Figure 1b**). Large chemical shifts were observed, many undergoing slow–intermediate exchange on the NMR timescale, indicating a strong interaction (low–micromolar affinity). The largest shifts were found to occur in the N–terminal region (Asp292–Val295), residues preceding the first β–strand (Glu305, Asp306), the first β–strand itself (Leu308–Cys311) and following residues, which are part of the second Zn finger

(Gly313, Asp315) (**Figure 1c**). Additionally, residues near the C–terminal were also perturbed (Val330, Trp335). These residues were mapped onto a generated I–TASSER homology model[43] of PHD1, and all these clustered to the same face of PHD1. Overlaying the H3 peptide bound NMR structure of the $PHD1_{KDM5B}$[13] with our homology model showed that the residues with the largest chemical shifts changes coincided with the peptide binding region of $PHD1_{KDM5B}$ (**Figure 1d**). Large shifts in Asp292, Tyr294, and their adjacent residues, not seen in studies with Asp292–Glu344 PHD1, indicate the importance of these residues in H3 binding. Similar trends have been observed in NMR studies of AIRE[10] and the $PHD1_{KDM5B}$[12,13]. In $PHD1_{KDM5B}$ large chemical shifts occur in the first β–sheet and residues before the C–terminal α–helix[12,13]. However, there are differences in the chemical shift perturbations of the N–terminal residues between the two studies, likely due to constructs and peptides used.

In the absence of the H3 ligand, the chemical shifts values of the N–terminal residues (Val288–Tyr294) of PHD1 suggest that they are unstructured (**Figure 1b**). However, upon addition of H3 10mer peptide we observe shifts of Asp292–Tyr294 away from unstructured chemical shift values, likely due to structural reorganization upon interaction of Asp292 and Tyr294 with the H3K4, and a consequent stabilization of this loop. Analysis of the chemical shifts of the Cα and Cβ peaks suggest that Phe290, Val291 and Leu293 shift towards a more α–helical conformation upon H3 binding. Ligand–induced structuring has been previously observed in the PHD domain of PHF20. Large conformational changes in the N–terminal region were observed as an N–terminal glutamate residue swings to the core of the PHD domain to interact with basic residues of the peptide ligand[8].

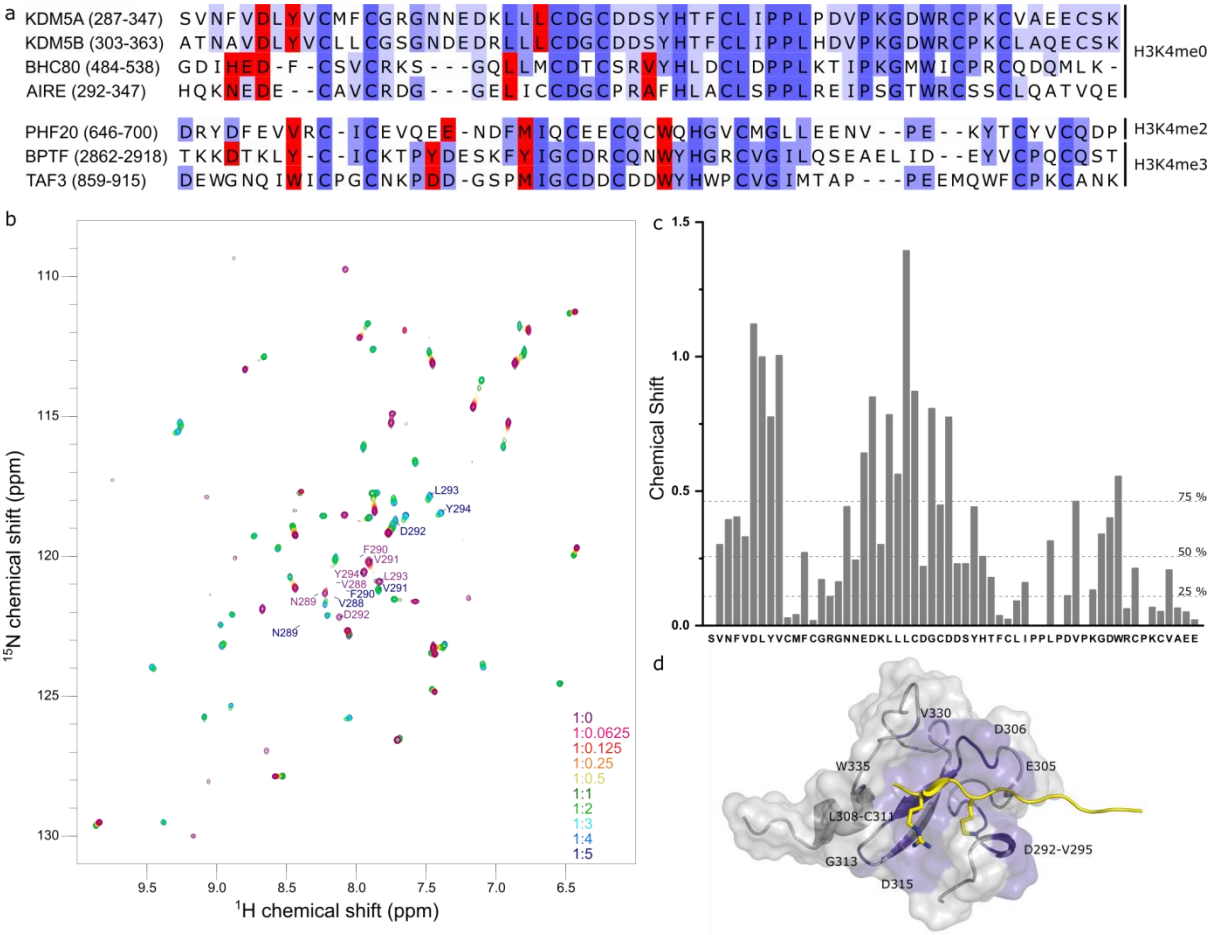

Figure 1. The N–terminal region of PHD1 undergoes large chemical shift perturbations upon H3 peptide binding. a) Sequence alignment of H3K4me0 and H3K4me2/3 preferring PHD1 domains. Residues highlighted in red interact with H3K4. Conserved residues are shown in blue. b) 2D HSQC spectra of H3 10mer titrations with ^{15}N labelled PHD1 (S287–E344). N–terminal residues of PHD1 are labelled with peaks from apo PHD1 in magenta and H3 10mer bound peaks in blue. Some peaks are labeled, but appear absent due to their low signal intensity. c) Chemical shift perturbations of peaks shown in b). 25th, 50th and 75th percentiles are indicated with dashed lines. d) I–TASSER homology model of PHD1$_{KDM5A}$ overlaid with a H3 peptide from PHD1$_{KDM5B}$ (PDB ID: 2MNZ) shown in yellow. Residues that are in the top 75th percentile shown in Fig 1c are highlighted in blue.

Differential engagement with methylated H3K4 peptides by PHD1

Methylation of H3K4 greatly impacts the affinity of the H3 peptide for PHD1 with an increase in the number of methyl groups on H3K4 resulting in decreased affinity[41]. Interestingly, $PHD1_{KDM5A}$ domain is still able to bind all three methylated states of H3K4 (**Table 1**), a feature distinct from several other PHD domains that engage unmodified H3 tails. For example AIRE[10], TRIM24[44], CHD4's PHD2[45], BHC80[9] and the PHD–like domain of DNMT3L[46] also show weak binding for methylated H3K4 peptides with K_d values measured to be >200 µM or non–binding for higher methylation states (H3K4me2 and me3). Even the similar $PHD1_{KDM5B}$ shows weaker binding (>80 µM for H3K4me2 and me3) to methylated H3K4 peptides[12,13]. The relatively high affinity of $PHD1_{KDM5A}$ for H3K4 methylated peptides could explain how allosteric stimulation of KDM5A's H3K4me3 demethylase activity initially occurs in H3K4me3 rich regions[42]. The ability of PHD1 to bind all three methylation states of H3K4 peptides with affinities of ≤39 µM, provides a unique opportunity to investigate how methylation is accommodated by this reader domain.

HSQC NMR titration measurements were performed with H3K4me1, H3K4me2 and H3K4me3 peptides (**Figure 2a, b, c**). For all three methylated peptides we see the presence of NMR signals indicating fast exchange on the NMR timescale, suggesting weaker interactions than with unmodified H3. However, H3K4me1 still contains a large number of signals in slow– intermediate exchange on the NMR timescale suggesting strong interactions, comparable to with unmodified H3. We observe that similar residues are engaged upon binding of unmodified and methylated H3 peptides, implying the binding site used is similar overall (**Figure 2d**). However, significant differences in the behavior of specific residues show alternate interactions are made with methylated peptides.

When the H3K4me1 peptide is bound, the majority of peak shifts are similar to those on binding to the unmodified peptide (**Figure 2d, e; pink bars**). However, with mono–methylation some residues are affected to a lesser degree with the largest decreases in chemical shift changes occurring for residues Val291–Leu293, which includes the H3K4

binding pocket residue Asp292 (**Figure 2f**). Interestingly, Tyr294 and Leu310 show relatively little change in chemical shift perturbations suggesting mono–methylation does not affect their interaction with the H3K4 residue.

Smaller chemical shift changes, relative to when the unmodified H3 peptide is bound, are observed with binding of the H3K4me2 peptide. The largest reduction in chemical shifts, relative to the unmodified H3 peptide, are in the Val291–Val295 region (**Figure 2d,e green bars**). Our observations suggest that the presence of two methyl groups causes reduced interactions with the H3K4 interacting residues Asp292 and Tyr294. These changes are in contrast to relatively small changes in the conserved Leu310, which appears to be unaffected by H3K4 di–methylation.

Binding of H3K4me3 causes a large reduction in the chemical shift perturbations, relative to unmodified H3. The largest differences in chemical shift changes between the unmodified and tri–methylated ligand occur in residues that form the H3K4 binding pocket (Val291–Tyr294) and in residues around the first β–strand (E305–D315) (**Figure 2d, e; blue bars**). The reduced interaction of the Val291–Tyr294 region with the peptide is likely due to the bulky nature of the H3K4me3 side chain in the H3K4 binding pocket. The biggest changes occur with Asp292, likely due to the inability of H3K4me3 to form a hydrogen bond with Asp292. In contrast to Asp292, Tyr294 and Leu310 show smaller differences in the magnitudes of their chemical shift perturbations between the tri–methylated and unmodified ligand, suggesting that these residues are more likely to interact with the alkyl chain of H3K4, rather than its ε–amino group.

Interestingly, upon H3K4me3 binding, three residues (Cys296, Met297 and Cys299) undergo increased perturbation compared to unmodified H3 binding. These residues are part of the first Zn–finger and are positioned on a loop underneath the H3K4 binding pocket (**Figure 2g**). We hypothesize that upon binding of the H3K4me3 group, the chemical environment of these residues is perturbed due to the structural changes needed to

accommodate the bulky group and allowing it to occupy the H3K4 binding pocket (**Figure 2f**).

Together our NMR data indicates that, of the H3K4 binding pocket residues, Asp292 is the most sensitive to the methylation state of the peptides as we see much larger decreases in the chemical shift perturbations of this amino acid as the methylation state increases. This is potentially due to the flexible nature of the N–terminal loop that harbors this residue, as well as modulation of a hydrogen bond between the ε–amino group of H3K4 and Asp292. Large changes in Tyr294 are only observed when di–methyl K4 is present and it is only when tri–methyl K4 is present that significant changes in Leu310 and adjacent residues are observed. Interestingly, with H3K4me3 bound there are still large chemical shift changes in residues, such as Leu310, which suggests it makes quite tight interactions with methylated H3K4 peptides.

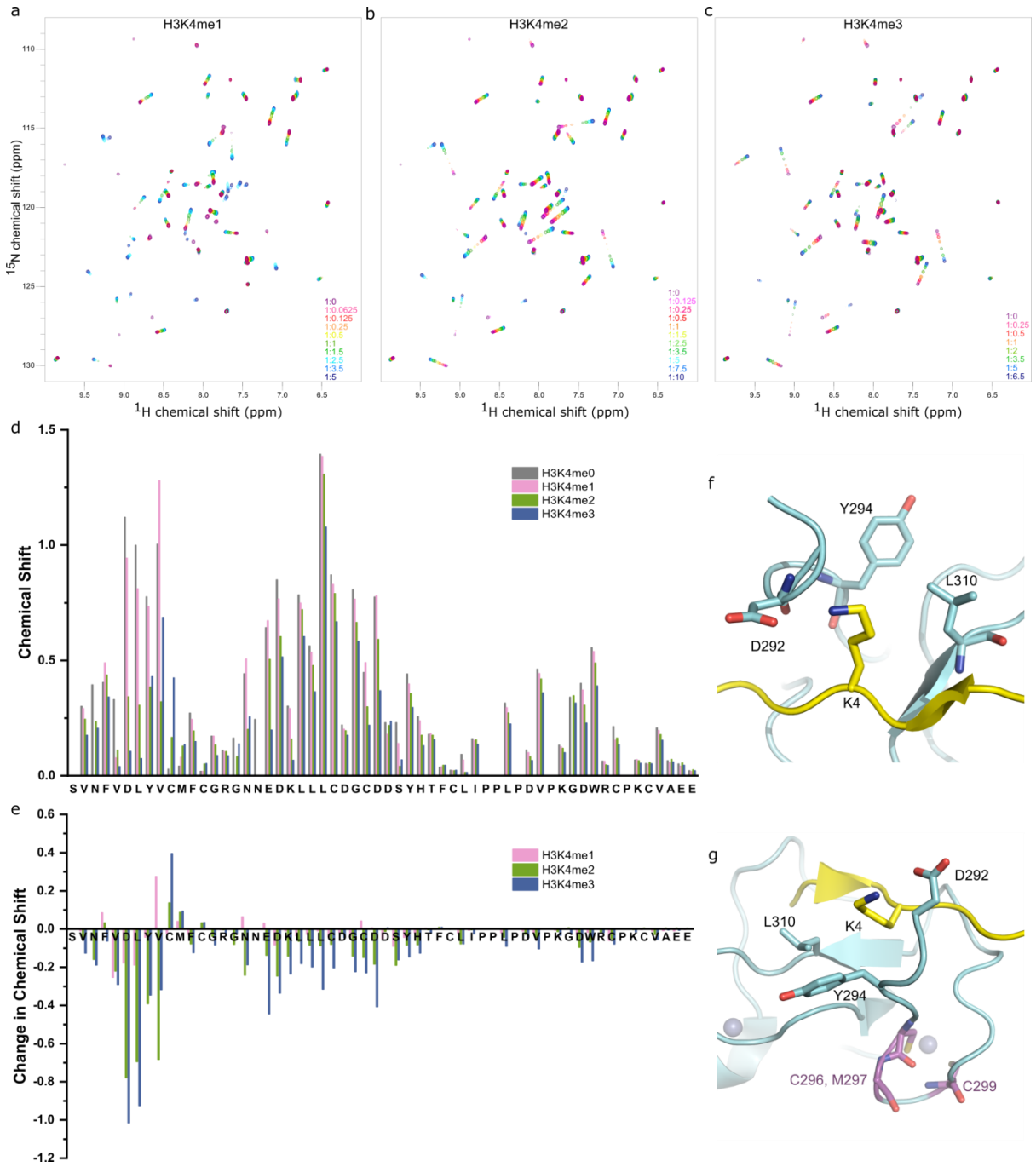

Figure 2. Binding to differently methylated H3 peptides causes reduced interaction with N–terminal residues. a–c) HSQC spectra of H3 10mer peptide titrations with ^{15}N labelled PHD1 (S287–E344) and a) H3K4me1, b) H3K4me2 and c) H3K4me3. d) Chemical shift perturbation of peaks upon addition of H3K4me1, me2 and me3 10mer peptides. e) Change in chemical shift perturbations shown in d) relative to shifts in H3K4me0. f) H3K4 binding pocket in $PHD1_{KDM5B}$ with $PHD1_{KDM5A}$'s residue numbering (PDB ID: 2MNZ). g) Residues undergoing increased perturbation upon H3K4me3 binding are shown in magenta. PHD1 domain of KDM5B was used, but with $PHD1_{KDM5A}$'s numbering (PDB ID: 2MNZ).

Assessing the interactions of H3K4 binding pocket residues

Our NMR data have provided insights into the interactions of the H3K4 binding pocket and differently methylated H3 peptides. In order to further assess the role of the H3K4 binding pocket residues (Asp292, Tyr294 and Leu310) in H3 peptide binding and methyl recognition we mutated these residues and measured H3 peptide binding to PHD1.

Mutation of Asp292 to Ala decreases the affinity of PHD1 for H3 ~6–fold relative to WT (**Table 1**). It also reduces binding to H3K4me1/2/3 peptides, with a 4–fold reduction for the interaction with H3K4me1 and ~2–fold reduction for higher methylation states. This decreased dependence on the presence of the carboxylate for binding higher methylation states of the peptide is consistent with a decrease in hydrogen bonding capacity of H3K4 and consistent with our chemical shift perturbation measurements (**Figure 2**).

D292N PHD1 has a similar affinity to D292A with similar fold–reductions for the unmodified and H3K4me1 peptides likely due to the removal of the electrostatic interaction between the Asp292 and H3K4 side chains (**Table 1**). K_d values for binding of the H3K4me2 peptide to the D292N mutant differ from those of D292A, but overall show a much reduced affinity relative to the WT PHD1. However, the K_d for H3K4me3 binding to the D292N mutant is similar to WT values, suggesting that the negative charge of the aspartate is not as important in H3K4me3 binding, but that other side chain contacts likely are.

When Tyr294 was mutated to an Ala, a ~15–fold decrease in affinity for the unmodified H3 peptide was observed as well as a reduced affinity for methylated peptides, consistent with our NMR data (**Table 1 and Figure 2**). Unlike the Y294A mutation, replacement of this residue with Phe diminishes binding of unmodified and mono–methylated peptides by <3–fold, with a minimal impact on binding of di– and tri–methylated peptides. These findings suggest the importance of hydrophobic and π–cation interactions between Lys4 and the aromatic ring of Tyr294. This is supported by the NMR structure of $PHD1_{KDM5B}$, as the ε–CH_2 of Lys4 is directed towards the Tyr294 ring (**Figure 2f**) consistent with preferred engagement

of the ε–CH_2 group of lysine in π–cation interactions [47,48]. In addition, tri–methylated lysine has been shown to enhance these interactions with aromatic residues[49].

Table 1. Binding affinities of PHD1 H3K4 pocket variants to H3 peptides

PHD1 variant	K_d (μM)			
	H3K4me0	H3K4me1	H3K4me2	H3K4me3
WT	0.82 ± 0.09[a]	3.86 ± 0.76	15.0 ± 3.0	38.5 ± 6.8
D292A	4.91 ± 0.10[a]	15.5 ± 3.8	29.5 ± 5.3	83.9 ± 25.5
D292N	5.13 ± 0.46[a]	15.9 ± 1.8	50.1 ± 7.0	38.2 ± 3.0
Y294A	12.0 ± 0.8[a]	21.6 ± 3.0	95.4 ± 12.3	67.7 ± 22.6
Y294F	2.59 ± 0.20[a]	9.06 ± 2.25	17.8 ± 1.4	57.8 ± 8.7
L310A	48.4 ± 4.1[a]	>100	>100	>100

[a] Indicates measurements were performed via direct FP

L310A shows greatly reduced binding affinity for the unmodified and methylated H3 peptides, with a nearly 60–fold decrease in affinity for the unmodified H3 peptide. This is consistent with observations of a large chemical shift perturbation of Leu310 upon peptide binding. The equivalent residue in $PHD1_{KDM5B}$ (Leu326) interacts both with H3K4 and H3R2 residues in the H3 peptide, and as such is a major contributor to peptide binding.

Together our data indicate that, of the K4 binding pocket residues, Leu310 contributes the most to the binding affinity, followed by Tyr294 and Asp292. These data suggest a finely tuned binding site with varying, methylation–dependent, contributions to H3 binding and H3K4 methyl discrimination. However, the contributions of these residues to binding may not be conserved between KDM5 family PHD1 domains. Mutations of H3K4 binding pocket residues in $PHD1_{KDM5B}$, Y310 and L326 (Y294 and L310 in KDM5A) resulted in ~2 and 4–fold lower affinity for unmodified H3 peptides was compared to WT[13]. In contrast, we observe much larger changes upon mutation of these residues, ~15 to 60–fold change, in $PHD1_{KDM5A}$, suggesting differential interactions with H3 exist with the PHD1 domains of KDM5A and KDM5B, despite their high sequence similarity.

The role of H3 peptide interacting residues in PHD1

We have shown previously that interaction of H3R2 with PHD1 is a major contributor to the high affinity of PHD1 for H3[41]. Mutation of the conserved R2 interacting residues Asp312 and Asp315 greatly impacts binding, with Asp312 being essential for binding. Additionally, we have previously shown that the conserved Trp residue in PHD domains (**Figure 1a**), Trp335 in PHD1, likely interacts with the N–terminus of the peptide. However, it is unknown what contributions, if any, other residues of H3 might have to the overall binding affinity. To address this question, we mutated several H3 interacting residues predicted by our homology model and the structural information available for $PHD1_{KDM5B}$[13] (**Figure 1**), and subsequently measured the affinity of mutants for the H3 peptide.

Val330 is predicted to form hydrophobic interactions with H3T3 (**Figure 3b**). Mutating this residue to an alanine reduced the affinity 3.5–fold (**Figure 3a**). Similar K_d values of the WT and V330A PHD1 towards methylated H3 peptides suggest that the interaction between Val330 and H3T3 has a significant contribution only to the binding of the highest affinity unmodified H3 peptide ligand. Glu305 is predicted to hydrogen bond to both H3T3 and H3Q5 (**Figure 3b**). Mutation of this residue to Ala results in ~6–fold reduction in affinity for both unmodified and mono–methylated H3K4 (**Figure 3a, b**) suggesting this residue makes significant interactions with the H3 peptide. The smaller decrease in affinity observed with H3K4me2 and me3 suggests a decreased dependence on interactions of these peptides with Glu305. Val295 and Asn303 in PHD1 are predicted to form hydrophobic interactions with H3T6 (**Figure 3b**). Mutating Val295 and Asn303 to alanine resulted in a ~2 and ~3–fold decrease in affinity for unmodified H3 peptide, respectively. Minor perturbations in the affinity of both V295A and N303A mutants towards methylated peptides was observed, suggesting that like Val330, Val295 and Asn303 only contribute to binding of unmodified ligand and not the side–chain of H3K4. Similar perturbations were observed in KDM5B where mutation of V311A (V295A in KDM5A) resulted in a modest decrease in affinity.

Collectively, our data suggest that H3 residues A1, R2 and K4 are the main determinants of H3 peptide binding, but interactions with H3T3 and H3T6 do contribute to a lesser extent. Interestingly, Glu305, predicted to interact with H3T3 and H3Q5, was found to have significant contributions to affinity for all peptides, highlighting the importance of this residue in interacting with the H3 tail.

Mutations within the PHD1 domain have been observed in various cancers. Our data could suggest their role in aberrant KDM5A function. Examples include Y294F found in a bladder carcinoma; D292N in stomach adenocarcinoma and CNS glioma; E305K in breast invasive ductal carcinoma and head and neck squamous cell carcinoma; and V330M in cutaneous celanoma (COSMIC and cBioPortal databases[50–52]). We observed reduced binding capacity for low methylation–state H3K4 peptides with D292N and Y294F mutant PHD1 (**Table 1**). We have also shown that E305 is an important H3 binding residue and the introduction of a positive lysine residue, as in the E305K disease mutation, would affect PHD1 interactions with H3.

a

PHD1 variant	K_d (μM)				H3 Interacting residue
	H3K4me0	H3K4me1	H3K4me2	H3K4me3	
WT	0.82 ± 0.09[a]	3.86 ± 0.76	15.0 ± 3.0	38.5 ± 6.8	N/A
V330A	2.88 ± 0.11[a]	5.97 ± 1.09	13.3 ± 2.7	23.3 ± 5.1	T3
E305A	5.14 ± 0.34[a]	24.1 ± 4.7	69.8 ± 11.3	125.1 ± 35.3	T3/Q5
V295A	1.39 ± 0.08[a]	3.67 ± 1.02	12.5 ± 1.4	26.0 ± 4.6	T6
N303A	2.77 ± 0.20[a]	5.61 ± 1.31	23.0 ± 3.3	36.5 ± 10.5	T6

[a]Indicates measurements were performed via direct FP

b

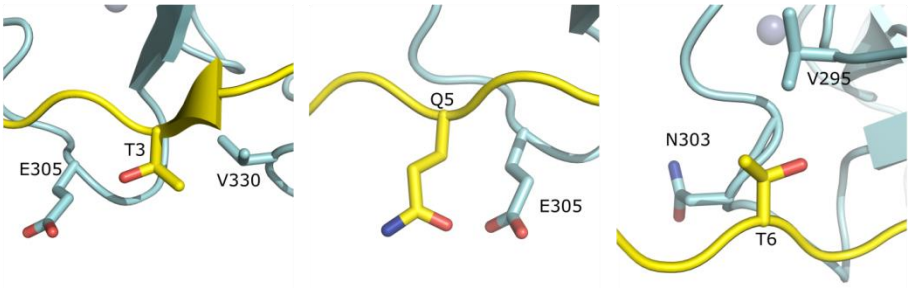

Figure 3. Binding affinities of PHD1 peptide binding site variants for methylated H3 peptides. a) K_d values of PHD1 peptide binding pocket variants binding to differently methylated H3K4 10mer peptides. b) Location of residues mutated in the study, shown in the structure of the PHD1 domain of KDM5B (PDB ID: 2MNZ). $PHD1_{KDM5B}$ is shown in cyan, the H3 peptide is shown in yellow.

Summary

Overall, our findings provide an understanding of how $PHD1_{KDM5A}$ recognizes H3 tail residues and discriminates against H3K4 methylation. Using NMR, we observe that an initially unstructured N–terminal region interacts strongly with H3 peptides and becomes more structured upon ligand binding (**Figure 1**). Significantly reduced interactions of the N–terminal residues with methylated H3K4 peptides further highlights the importance of this region in regulating the methylation selectivity in PHD1. We also identify the interactions that allow PHD1 to interact with relatively high affinity to methylated H3K4 peptides, a property that makes $PHD1_{KDM5A}$, so far, unique when compared to related PHD domains. Given the allosteric role of this reader domain in KDM5A demethylase activity, our findings also provide insights into how mutations in this domain would impact allosteric ligand binding and therefore modulate activity of KDM5A. The greater understanding of the structural features of PHD1 and H3 binding provided here will facilitate development of PHD1–targeting small molecule modulators of KDM5A for use as chemical tool compounds.

Acknowledgments

We would like to thank Nektaria Petronikolou and Fatima Ugur for their comments on the paper.

Funding Sources

This work is supported by National Institutes of Health (R01 GM114044 and R01 GM114044-03S1)

References

(1) Musselman, C. A.; Lalonde, M.–E.; Côté, J.; Kutateladze, T. G. Perceiving the Epigenetic Landscape through Histone Readers. *Nat. Struct. Mol. Biol.* **2012**, *19* (12), 1218–1227. https://doi.org/10.1038/nsmb.2436.

(2) Sanchez, R.; Zhou, M.–M. The PHD Finger: A Versatile Epigenome Reader. *Trends Biochem. Sci.* **2011**, *36* (7), 364–372. https://doi.org/10.1016/j.tibs.2011.03.005.

(3) Dhar, S. S.; Lee, S.–H.; Kan, P.–Y.; Voigt, P.; Ma, L.; Shi, X.; Reinberg, D.; Lee, M. G. Trans–Tail Regulation of MLL4–Catalyzed H3K4 Methylation by H4R3 Symmetric Dimethylation Is Mediated by a Tandem PHD of MLL4. *Genes Dev.* **2012**, *26* (24), 2749–2762. https://doi.org/10.1101/gad.203356.112.

(4) Liu, Y.; Qin, S.; Chen, T.–Y.; Lei, M.; Dhar, S. S.; Ho, J. C.; Dong, A.; Loppnau, P.; Li, Y.; Lee, M. G.; et al. Structural Insights into Trans–Histone Regulation of H3K4 Methylation by Unique Histone H4 Binding of MLL3/4. *Nat. Commun.* **2019**, *10* (1), 36. https://doi.org/10.1038/s41467–018–07906–3.

(5) Li, H.; Ilin, S.; Wang, W.; Duncan, E. M.; Wysocka, J.; Allis, C. D.; Patel, D. J. Molecular Basis for Site–Specific Read–out of Histone H3K4me3 by the BPTF PHD Finger of NURF. *Nature* **2006**, *442* (7098), 91–95. https://doi.org/10.1038/nature04802.

(6) van Ingen, H.; van Schaik, F. M. A.; Wienk, H.; Ballering, J.; Rehmann, H.; Dechesne, A. C.; Kruijzer, J. A. W.; Liskamp, R. M. J.; Timmers, H. T. M.; Boelens, R. Structural Insight into the Recognition of the H3K4me3 Mark by the TFIID Subunit TAF3. *Structure* **2008**, *16* (8), 1245–1256. https://doi.org/10.1016/j.str.2008.04.015.

(7) Hughes, R. M.; Wiggins, K. R.; Khorasanizadeh, S.; Waters, M. L. Recognition of Trimethyllysine by a Chromodomain Is Not Driven by the Hydrophobic Effect. *Proc. Natl. Acad. Sci.* **2007**, *104* (27), 11184–11188. https://doi.org/10.1073/pnas.0610850104.

(8) Klein, B. J.; Wang, X.; Cui, G.; Yuan, C.; Botuyan, M. V.; Lin, K.; Lu, Y.; Wang, X.; Zhao, Y.; Bruns, C. J.; et al. PHF20 Readers Link Methylation of Histone H3K4 and P53 with H4K16 Acetylation. *Cell Rep.* **2016**, *17* (4), 1158–1170. https://doi.org/10.1016/j.celrep.2016.09.056.

(9) Lan, F.; Collins, R. E.; De Cegli, R.; Alpatov, R.; Horton, J. R.; Shi, X.; Gozani, O.; Cheng, X.; Shi, Y. Recognition of Unmethylated Histone H3 Lysine 4 Links BHC80 to LSD1–Mediated Gene Repression. *Nature* **2007**, *448* (7154), 718–722. https://doi.org/10.1038/nature06034.

(10) Org, T.; Chignola, F.; Hetényi, C.; Gaetani, M.; Rebane, A.; Liiv, I.; Maran, U.; Mollica, L.; Bottomley, M. J.; Musco, G.; et al. The Autoimmune Regulator PHD Finger Binds to Non–Methylated Histone H3K4 to Activate Gene Expression. *EMBO Rep.* **2008**, *9* (4), 370–376. https://doi.org/10.1038/sj.embor.2008.11.

(11) Chakravarty, S.; Zeng, L.; Zhou, M.–M. Structure and Site–Specific Recognition of Histone H3 by the PHD Finger of Human Autoimmune Regulator. *Structure* **2009**, *17* (5), 670–679. https://doi.org/10.1016/j.str.2009.02.017.

(12) Klein, B. J.; Piao, L.; Xi, Y.; Rincon–Arano, H.; Rothbart, S. B.; Peng, D.; Wen, H.; Larson, C.; Zhang, X.; Zheng, X.; et al. The Histone–H3K4–Specific Demethylase KDM5B Binds to Its Substrate and Product through Distinct PHD Fingers. *Cell Rep.*

2014, *6* (2), 325–335. https://doi.org/10.1016/j.celrep.2013.12.021.

(13) Zhang, Y.; Yang, H.; Guo, X.; Rong, N.; Song, Y.; Xu, Y.; Lan, W.; Zhang, X.; Liu, M.; Xu, Y.; et al. The PHD1 Finger of KDM5B Recognizes Unmodified H3K4 during the Demethylation of Histone H3K4me2/3 by KDM5B. *Protein Cell* **2014**, *5* (11), 837–850. https://doi.org/10.1007/s13238–014–0078–4.

(14) Mansfield, R. E.; Musselman, C. A.; Kwan, A. H.; Oliver, S. S.; Garske, A. L.; Davrazou, F.; Denu, J. M.; Kutateladze, T. G.; Mackay, J. P. Plant Homeodomain (PHD) Fingers of CHD4 Are Histone H3–Binding Modules with Preference for Unmodified H3K4 and Methylated H3K9. *J. Biol. Chem.* **2011**, *286* (13), 11779–11791. https://doi.org/10.1074/jbc.M110.208207.

(15) Wang, G. G.; Song, J.; Wang, Z.; Dormann, H. L.; Casadio, F.; Li, H.; Luo, J.–L.; Patel, D. J.; Allis, C. D. Haematopoietic Malignancies Caused by Dysregulation of a Chromatin–Binding PHD Finger. *Nature* **2009**, *459* (7248), 847–851. https://doi.org/10.1038/nature08036.

(16) Teng, Y.–C.; Lee, C.–F.; Li, Y.–S.; Chen, Y.–R.; Hsiao, P.–W.; Chan, M.–Y.; Lin, F.–M.; Huang, H.–D.; Chen, Y.–T.; Jeng, Y.–M.; et al. Histone Demethylase RBP2 Promotes Lung Tumorigenesis and Cancer Metastasis. *Cancer Res.* **2013**, *73* (15), 4711–4721. https://doi.org/10.1158/0008–5472.CAN–12–3165.

(17) Shen, X.; Zhuang, Z.; Zhang, Y.; Chen, Z.; Shen, L.; Pu, W.; Chen, L.; Xu, Z. JARID1B Modulates Lung Cancer Cell Proliferation and Invasion by Regulating P53 Expression. *Tumor Biol.* **2015**, *36* (9), 7133–7142. https://doi.org/10.1007/s13277–015–3418–y.

(18) Bayo, J.; Tran, T. A.; Wang, L.; Peña–Llopis, S.; Das, A. K.; Martinez, E. D. Jumonji Inhibitors Overcome Radioresistance in Cancer through Changes in H3K4 Methylation at Double–Strand Breaks. *Cell Rep.* **2018**, *25* (4), 1040–1050.e5. https://doi.org/10.1016/j.celrep.2018.09.081.

(19) Wang, L.; Mao, Y.; Du, G.; He, C.; Han, S. Overexpression of JARID1B Is Associated with Poor Prognosis and Chemotherapy Resistance in Epithelial Ovarian Cancer. *Tumor Biol.* **2015**, *36* (4), 2465–2472. https://doi.org/10.1007/s13277–014–2859–z.

(20) Liu, X.; Secombe, J. The Histone Demethylase KDM5 Activates Gene Expression by Recognizing Chromatin Context through Its PHD Reader Motif. *Cell Rep.* **2015**, *13* (10), 2219–2231. https://doi.org/10.1016/j.celrep.2015.11.007.

(21) Wu, L.; Cao, J.; Cai, W. L.; Lang, S. M.; Horton, J. R.; Jansen, D. J.; Liu, Z. Z.; Chen, J. F.; Zhang, M.; Mott, B. T.; et al. KDM5 Histone Demethylases Repress Immune Response via Suppression of STING. *PLOS Biol.* **2018**, *16* (8), e2006134. https://doi.org/10.1371/journal.pbio.2006134.

(22) Li, J.; Wan, X.; Qiang, W.; Li, T.; Huang, W.; Huang, S.; Wu, D.; Li, Y. MiR–29a Suppresses Prostate Cell Proliferation and Induces Apoptosis via KDM5B Protein Regulation. *Int. J. Clin. Exp. Med.* **2015**, *8* (4), 5329–5339. https://doi.org/PMC4483968.

(23) Roesch, A.; Fukunaga–Kalabis, M.; Schmidt, E. C.; Zabierowski, S. E.; Brafford, P. A.; Vultur, A.; Basu, D.; Gimotty, P.; Vogt, T.; Herlyn, M. A Temporarily Distinct Subpopulation of Slow–Cycling Melanoma Cells Is Required for Continuous Tumor Growth. *Cell* **2010**, *141* (4), 583–594. https://doi.org/10.1016/j.cell.2010.04.020.

(24) Rondinelli, B.; Rosano, D.; Antonini, E.; Frenquelli, M.; Montanini, L.; Huang, D.; Segalla, S.; Yoshihara, K.; Amin, S. B.; Lazarevic, D.; et al. Histone Demethylase JARID1C Inactivation Triggers Genomic Instability in Sporadic Renal Cancer. *J. Clin. Invest.* **2015**, *125* (12), 4625–4637. https://doi.org/10.1172/JCI81040.

(25) Li, N.; Dhar, S. S.; Chen, T.–Y.; Kan, P.–Y.; Wei, Y.; Kim, J.–H.; Chan, C.–H.; Lin, H.–K.; Hung, M.–C.; Lee, M. G. JARID1D Is a Suppressor and Prognostic Marker of Prostate Cancer Invasion and Metastasis. *Cancer Res.* **2016**, *76* (4), 831–843. https://doi.org/10.1158/0008–5472.CAN–15–0906.

(26) Pfister, S. X.; Ashworth, A. Marked for Death: Targeting Epigenetic Changes in Cancer. *Nat. Rev. Drug Discov.* **2017**, *16* (4), 241–263. https://doi.org/10.1038/nrd.2016.256.

(27) Rasmussen, P. B.; Staller, P. The KDM5 Family of Histone Demethylases as Targets in Oncology Drug Discovery. *Epigenomics* **2014**, *6* (3), 277–286. https://doi.org/10.2217/epi.14.14.

(28) Han, M.; Xu, W.; Cheng, P.; Jin, H.; Wang, X. Histone Demethylase Lysine Demethylase 5B in Development and Cancer. *Oncotarget* **2017**, *8* (5). https://doi.org/10.18632/oncotarget.13858.

(29) Paroni, G.; Bolis, M.; Zanetti, A.; Ubezio, P.; Helin, K.; Staller, P.; Gerlach, L. O.; Fratelli, M.; Neve, R. M.; Terao, M.; et al. HER2–Positive Breast–Cancer Cell Lines Are Sensitive to KDM5 Inhibition: Definition of a Gene–Expression Model for the Selection of Sensitive Cases. *Oncogene* **2019**, *38* (15), 2675–2689. https://doi.org/10.1038/s41388–018–0620–6.

(30) Yamamoto, S.; Wu, Z.; Russnes, H. G.; Takagi, S.; Peluffo, G.; Vaske, C.; Zhao, X.; Moen Vollan, H. K.; Maruyama, R.; Ekram, M. B.; et al. JARID1B Is a Luminal Lineage–Driving Oncogene in Breast Cancer. *Cancer Cell* **2014**, *25* (6), 762–777. https://doi.org/10.1016/j.ccr.2014.04.024.

(31) Jensen, L. R.; Amende, M.; Gurok, U.; Moser, B.; Gimmel, V.; Tzschach, A.; Janecke, A. R.; Tariverdian, G.; Chelly, J.; Fryns, J.–P.; et al. Mutations in the JARID1C Gene, Which Is Involved in Transcriptional Regulation and Chromatin Remodeling, Cause X–Linked Mental Retardation. *Am. J. Hum. Genet.* **2005**, *76* (2), 227–236. https://doi.org/10.1086/427563.

(32) Iwase, S.; Lan, F.; Bayliss, P.; de la Torre–Ubieta, L.; Huarte, M.; Qi, H. H.; Whetstine, J. R.; Bonni, A.; Roberts, T. M.; Shi, Y. The X–Linked Mental Retardation Gene SMCX/JARID1C Defines a Family of Histone H3 Lysine 4 Demethylases. *Cell*

2007, *128* (6), 1077–1088. https://doi.org/10.1016/j.cell.2007.02.017.

(33) Vinogradova, M.; Gehling, V. S.; Gustafson, A.; Arora, S.; Tindell, C. A.; Wilson, C.; Williamson, K. E.; Guler, G. D.; Gangurde, P.; Manieri, W.; et al. An Inhibitor of KDM5 Demethylases Reduces Survival of Drug–Tolerant Cancer Cells. *Nat. Chem. Biol.* **2016**, *12* (7), 531–538. https://doi.org/10.1038/nchembio.2085.

(34) Johansson, C.; Velupillai, S.; Tumber, A.; Szykowska, A.; Hookway, E. S.; Nowak, R. P.; Strain–Damerell, C.; Gileadi, C.; Philpott, M.; Burgess–Brown, N.; et al. Structural Analysis of Human KDM5B Guides Histone Demethylase Inhibitor Development. *Nat. Chem. Biol.* **2016**, *12* (7), 539–545. https://doi.org/10.1038/nchembio.2087.

(35) McAllister, T. E.; England, K. S.; Hopkinson, R. J.; Brennan, P. E.; Kawamura, A.; Schofield, C. J. Recent Progress in Histone Demethylase Inhibitors. *J. Med. Chem.* **2016**, *59* (4), 1308–1329. https://doi.org/10.1021/acs.jmedchem.5b01758.

(36) Tumber, A.; Nuzzi, A.; Hookway, E. S.; Hatch, S. B.; Velupillai, S.; Johansson, C.; Kawamura, A.; Savitsky, P.; Yapp, C.; Szykowska, A.; et al. Potent and Selective KDM5 Inhibitor Stops Cellular Demethylation of H3K4me3 at Transcription Start Sites and Proliferation of MM1S Myeloma Cells. *Cell Chem. Biol.* **2017**, *24* (3), 371–380. https://doi.org/10.1016/j.chembiol.2017.02.006.

(37) Miyake, Y.; Itoh, Y.; Hatanaka, A.; Suzuma, Y.; Suzuki, M.; Kodama, H.; Arai, Y.; Suzuki, T. Identification of Novel Lysine Demethylase 5–Selective Inhibitors by Inhibitor–Based Fragment Merging Strategy. *Bioorg. Med. Chem.* **2019**, *27* (6), 1119–1129. https://doi.org/10.1016/j.bmc.2019.02.006.

(38) Cao, J.; Liu, Z.; Cheung, W. K. C.; Zhao, M.; Chen, S. Y.; Chan, S. W.; Booth, C. J.; Nguyen, D. X.; Yan, Q. Histone Demethylase RBP2 Is Critical for Breast Cancer Progression and Metastasis. *Cell Rep.* **2014**, *6* (5), 868–877. https://doi.org/10.1016/j.celrep.2014.02.004.

(39) Hinohara, K.; Wu, H.–J.; Vigneau, S.; McDonald, T. O.; Igarashi, K. J.; Yamamoto, K. N.; Madsen, T.; Fassl, A.; Egri, S. B.; Papanastasiou, M.; et al. KDM5 Histone Demethylase Activity Links Cellular Transcriptomic Heterogeneity to Therapeutic Resistance. *Cancer Cell* **2018**, *34* (6), 939–953.e9. https://doi.org/10.1016/j.ccell.2018.10.014.

(40) Sharma, S. V.; Lee, D. Y.; Li, B.; Quinlan, M. P.; Takahashi, F.; Maheswaran, S.; McDermott, U.; Azizian, N.; Zou, L.; Fischbach, M. A.; et al. A Chromatin–Mediated Reversible Drug–Tolerant State in Cancer Cell Subpopulations. *Cell* **2010**, *141* (1), 69–80. https://doi.org/10.1016/j.cell.2010.02.027.

(41) Torres, I. O.; Kuchenbecker, K. M.; Nnadi, C. I.; Fletterick, R. J.; Kelly, M. J. S.; Fujimori, D. G. Histone Demethylase KDM5A Is Regulated by Its Reader Domain through a Positive–Feedback Mechanism. *Nat. Commun.* **2015**, *6*, 6204. https://doi.org/10.1038/ncomms7204.

(42) Longbotham, J. E.; Chio, C. M.; Dharmarajan, V.; Trnka, M. J.; Torres, I. O.; Goswami, D.; Ruiz, K.; Burlingame, A. L.; Griffin, P. R.; Fujimori, D. G. Histone H3 Binding to the PHD1 Domain of Histone Demethylase KDM5A Enables Active Site Remodeling. *Nat. Commun.* **2019**, *10* (1), 94. https://doi.org/10.1038/s41467–018–07829–z.

(43) Roy, A.; Kucukural, A.; Zhang, Y. I–TASSER: A Unified Platform for Automated Protein Structure and Function Prediction. *Nat. Protoc.* **2010**, *5* (4), 725–738. https://doi.org/10.1038/nprot.2010.5.

(44) Tsai, W.–W.; Wang, Z.; Yiu, T. T.; Akdemir, K. C.; Xia, W.; Winter, S.; Tsai, C.–Y.; Shi, X.; Schwarzer, D.; Plunkett, W.; et al. TRIM24 Links a Non–Canonical Histone Signature to Breast Cancer. *Nature* **2010**, *468* (7326), 927–932. https://doi.org/10.1038/nature09542.

(45) Musselman, C. A.; Mansfield, R. E.; Garske, A. L.; Davrazou, F.; Kwan, A. H.; Oliver,

S. S.; O'Leary, H.; Denu, J. M.; Mackay, J. P.; Kutateladze, T. G. Binding of the CHD4 PHD2 Finger to Histone H3 Is Modulated by Covalent Modifications. *Biochem. J.* **2009**, *423* (2), 179–187. https://doi.org/10.1042/BJ20090870.

(46) Ooi, S. K. T.; Qiu, C.; Bernstein, E.; Li, K.; Jia, D.; Yang, Z.; Erdjument–Bromage, H.; Tempst, P.; Lin, S.–P.; Allis, C. D.; et al. DNMT3L Connects Unmethylated Lysine 4 of Histone H3 to de Novo Methylation of DNA. *Nature* **2007**, *448* (7154), 714–717. https://doi.org/10.1038/nature05987.

(47) Tatko, C. D.; Waters, M. L. The Geometry and Efficacy of Cation–π Interactions in a Diagonal Position of a Designed β–Hairpin. *Protein Sci.* **2009**, *12* (11), 2443–2452. https://doi.org/10.1110/ps.03284003.

(48) Tatko, C. D.; Waters, M. L. Comparison of C−H···π and Hydrophobic Interactions in a β–Hairpin Peptide: Impact on Stability and Specificity. *J. Am. Chem. Soc.* **2004**, *126* (7), 2028–2034. https://doi.org/10.1021/ja038258n.

(49) Hughes, R. M.; Waters, M. L. Influence of N –Methylation on a Cation−π Interaction Produces a Remarkably Stable β–Hairpin Peptide. *J. Am. Chem. Soc.* **2005**, *127* (18), 6518–6519. https://doi.org/10.1021/ja0507259.

(50) Tate, J. G.; Bamford, S.; Jubb, H. C.; Sondka, Z.; Beare, D. M.; Bindal, N.; Boutselakis, H.; Cole, C. G.; Creatore, C.; Dawson, E.; et al. COSMIC: The Catalogue Of Somatic Mutations In Cancer. *Nucleic Acids Res.* **2019**, *47* (D1), D941–D947. https://doi.org/10.1093/nar/gky1015.

(51) Gao, J.; Aksoy, B. A.; Dogrusoz, U.; Dresdner, G.; Gross, B.; Sumer, S. O.; Sun, Y.; Jacobsen, A.; Sinha, R.; Larsson, E.; et al. Integrative Analysis of Complex Cancer Genomics and Clinical Profiles Using the CBioPortal. *Sci. Signal.* **2013**, *6* (269), pl1–pl1. https://doi.org/10.1126/scisignal.2004088.

(52) Cerami, E.; Gao, J.; Dogrusoz, U.; Gross, B. E.; Sumer, S. O.; Aksoy, B. A.;

Jacobsen, A.; Byrne, C. J.; Heuer, M. L.; Larsson, E.; et al. The CBio Cancer Genomics Portal: An Open Platform for Exploring Multidimensional Cancer Genomics Data. *Cancer Discov.* **2012**, *2* (5), 401–404. https://doi.org/10.1158/2159–8290.CD–12–0095.